The Coherent Circle Hough Transform

T.J. Atherton and D.J. Kerbyson
Department of Computer Science,
University of Warwick, Coventry, UK.

Abstract

We introduce a novel formulation of the Circle Hough Transform that we call the Coherent Circle Hough Transform. The technique uses phase to code for radii of circles. The usual simplifications of the Circle Hough Transform (CHT) are used in which lines pointing away from edge points are plotted rather than circles. Intersections of these "spokes" accumulate edge magnitude, or edge "energy", near the centres of circles. We introduce the use of a complex accumulator space and allow each spoke to vary in phase along its length. The spokes are in phase near the centre of circles and out of phase elsewhere. The spokes generated by noise are in random phase and destructively interfere. We present results for an isolated circle with additive white Gaussian noise for both the conventional Energy CHT and the new Coherent CHT. The results demonstrate that the technique reduces the mean and variance of the background level in the accumulator array, that the peak to background level improves, and that the peak width is reduced improving localisation of circle centres.

1 Introduction

The extension we describe here is novel and builds on earlier work on the Circle Hough Transform (CHT) by many others (Duda 1972, Kimme 1975, Sklansky 1978, Ballard 1982, Davies 1988, Yuen 1989, Leavers 1992), and on work by the authors on fast implementations of the closely related "Spoke Filter" (Minor 1981, Atherton 1990). The use of phase is now accepted as important in other areas, notably stereo (eg Langley 1990, Wilson 1992), and motion (eg Langley 1992). The notion of coherent integration, using phase, is widely accepted, eg in radar, as a superior technique (in terms of noise behaviour) to non-coherent integration, using energy or magnitude alone (eg. Woodward 1964, Levanon 1988).

The technique we outline here has the advantages of more robust behaviour under additive noise, and sharper peaks in the accumulator array (Davies 1992), when compared with traditional energy based CHT's.

2 The Circle Hough Transform

2.1 The Origins of the Circle Hough Transform

The CHT (Duda 1972, Kimme 1975, Sklansky 1978, Ballard 1982, Davies 1988, Yuen 1990) aims to find circular patterns of a given radius R within images. The Hough Transform achieves this detection by a technique that is related to matched filtering of the image. Hough Transforms have a number of desirable features:

- they are integrative in nature
- quantifiable behaviour under noise
- can detect partially obscured or low contrast objects
- their computational complexity is known

BMVC 1993 doi:10.5244/C.7.27

The Standard CHT operates as follows: After edge detection of the image each edge point is taken as a centre of a circle of radius R drawn onto an accumulator array. Many constructed circles intersect leading to a large intensity peak in the accumulator array at, or near, the centre of the circle, Figure 1a illustrates this.

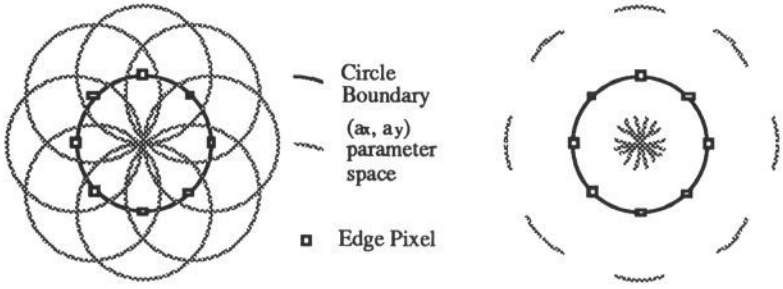

(a) Standard CHT *(b) Use of edge orientation*

Figure 1. The CHT showing the edge points and accumulator.

The CHT as described above may be carried out for a range of different radii. This leads to an accumulator array, or parameter space, that is three dimensional, the position of the centre and the radius, i.e. (**a**, R), where $\mathbf{a} = (a_x, a_y)$:

$$(x - a_x)^2 + (y - a_y)^2 = R^2 \qquad (1)$$

2.2 Modifications to the Standard CHT

Speed improvements, but not always performance improvements, to the CHT include:

- reducing the size of the image,
- reducing the range of radii considered,
- thresholding the edge image to reduce the edge point density
- plotting an arc (if edge direction is known) in the accumulator array
- plotting a single point for each radius under consideration

Figure 1b shows squares marking the positions of edge points, the candidate centre for a circle being at the intersection of the arcs. There will be one such accumulator array for each radius to be considered.

The CHT may be further enhanced by considering a range of radii simultaneously. This has the effect of reducing the dimensionality of the accumulator array from three to two, with significant implications for the implementation of the algorithm. The circles in the three dimensional accumulator array around an edge point are considered together to form a truncated cone, by using the edge direction circles may be collapsed to lines down the sides of this cone, Figure 2a. Projecting these lines onto two dimensions, Figure 2b, gives the "spoke" filter.

We consider a novel enhancement that replaces the CHT accumulator array with a complex accumulator array.

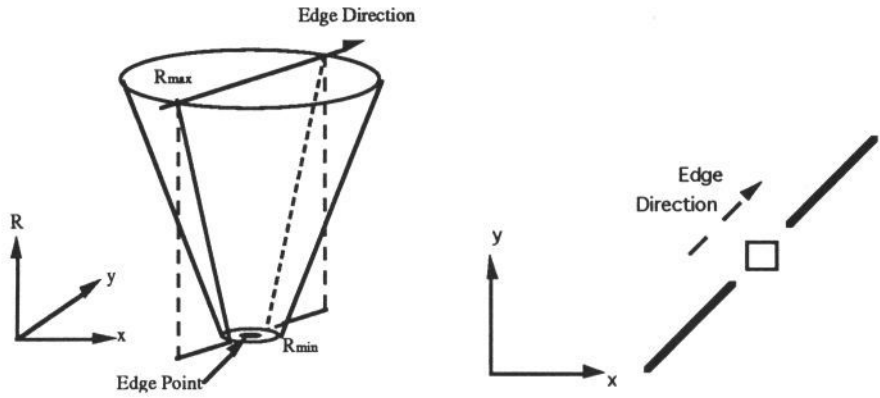

(a) the 3D accumulator array *(b) result of collapsing into a 2D array*

Figure 2. CHT Accumulator array for Multiple Radii using edge orientation

3 The Coherent Circle Hough Transform

The Coherent CHT uses phase to code for the radii. The technique uses a complex (in the sense of real and imaginary!) accumulator array. Edge points are projected along a line in the direction of the edge orientation. The projected edge points have a phase associated with them that is proportional to the distance travelled away from the edge point. As each edge point is projected its complex value is accumulated in the transform array. Edge points lying on a circle will have projections that intersect at a common point (ignoring noise effects and other errors), they will also be in phase (as the intersection is the same distance from all edge points on a circle). There is coherent integration of the edge points, from a circle, into the complex accumulator array. Edge projections from edges not on a circle, or from edges on another circle, will be in random phase and will not coherently integrate, they will tend to cancel. The centres of the circles are shown by the positions of the peaks in the magnitude of the accumulator array. The radius of a circle is the phase at the peak position.

We do not threshold edge points. Implicit in any thresholding is a decision: an edge point is discarded if its edge magnitude is weak, regardless of whether it lies on a circle or not. The processing flow has the form shown in Figure 3.

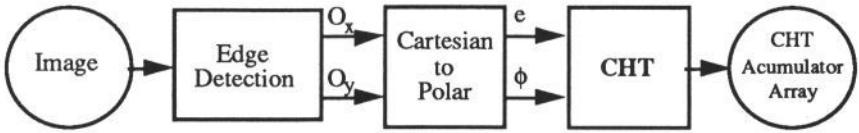

Figure 3 - The processing flow used to generate the CHT accumulator array.

The edge detected image is $\mathbf{O}(\mathbf{x}) = \left(O_x(\mathbf{x}), O_y(\mathbf{x})\right)^T$, which has magnitude $e(\mathbf{x}) = \|\mathbf{O}(\mathbf{x})\|$ and orientation $\varphi(\mathbf{x}) = \arg(\mathbf{O}(\mathbf{x}))$, with the unit vectors in these directions being $\hat{\mathbf{O}}(\mathbf{x})$. For the set of points X in the image I, the CHT accumulator space is initially:

$$H(\mathbf{x}) = 0 \quad \forall \mathbf{x} \in X \tag{2}$$

The Energy CHT, with the "spoke" enhancements described above, generates an accumulator array holding the values:

$$H_E(\mathbf{x}) = \sum_{\mathbf{x}' \in S(\mathbf{x})} e(\mathbf{x}') \tag{3}$$

where $S(\mathbf{x})$ is the set of points that lie within $R_{\min}$ and $R_{\max}$ of $\mathbf{x}$ and that have an edge orientation that points to or from $\mathbf{x}$, i.e.:

$$S(\mathbf{x}) = \left\{ \mathbf{w}; \left\| \left(\mathbf{I} - \hat{\mathbf{O}}(\mathbf{w}) \hat{\mathbf{O}}^T(\mathbf{w}) \right) (\mathbf{w} - \mathbf{x}) \right\| \leq 1, R_{\min} \leq \|(\mathbf{w} - \mathbf{x})\| \leq R_{\max} \right\} \tag{4}$$

The Coherent CHT generates an accumulator array in a similar way except that the accumuator array is complex:

$$H_C(\mathbf{x}) = \sum_{\mathbf{x}' \in S(\mathbf{x})} e(\mathbf{x}') \exp\left[-2\pi i u_0 \|\mathbf{x} - \mathbf{x}'\| \right] \tag{5}$$

The frequency of the sinusoid is such that one wavelength fits into the range between the maximum and minimum radii, i.e.:

$$u_0 = \left(R_{Max} - R_{Min} \right)^{-1} \tag{6}$$

4 Results

We report and compare the behaviours of the Energy and Coherent CHTs as the noise variance in the original image is varied. The images used are 128 by 128 pixels. In the centre of the image is a single circle of radius 16 pixels, it has a grey-level of 160 on a background of 96. In some experiments the circle is absent. The parameters to the Energy and Coherent CHT are R_{min}=8 pixels and R_{max}=24 pixels. The added noise in all cases is zero-mean and Gaussian.

The results reported fall into three groups:

1) Behaviour of Energy and Coherent CHT as noise variance in the input image (which does not contain a circle) is increased.
2) Behaviour of Energy and Coherent CHT as noise variance in the input image, containing a circle, is increased.
3) Energy and Coherent CHT accumulator arrays from a circle image.

4.1 Noise tests

In the first set of results the circle is absent. Figure 4 shows the mean and variance of the responses in the Energy and Coherent CHT accumulator arrays as the noise variance in the original image is increased.

4.2 Noisy image tests

In this set of results the circle is present. Figure 5a shows the ratio of the peak value to the mean of the accumulator array plotted against input image noise variance for the Energy and Coherent CHT's. Figure 5b shows the signal to noise power ratio in the accumulator arrays. These are measures of how far above the plateau the peaks stand.

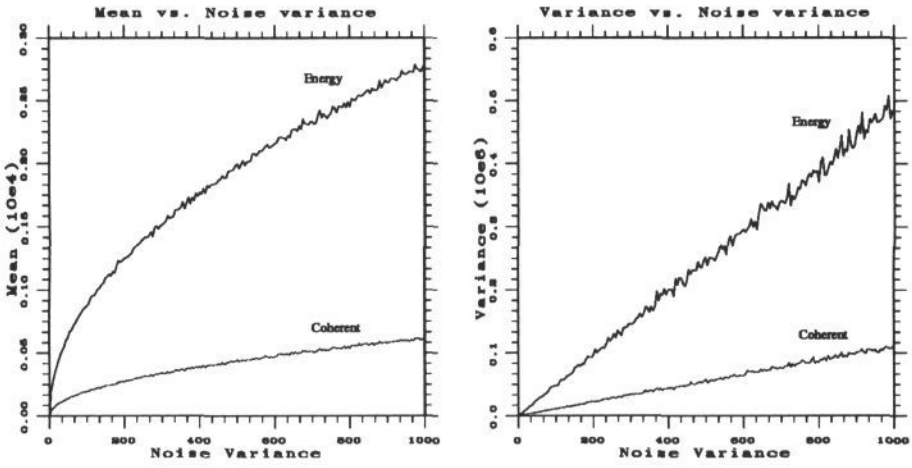

(a) Mean of accumulator arrays *(b) Variance of accumulator arrays*

Figure 4. Comparison of Energy and Coherent CHT responses to noise alone v. image noise variance.

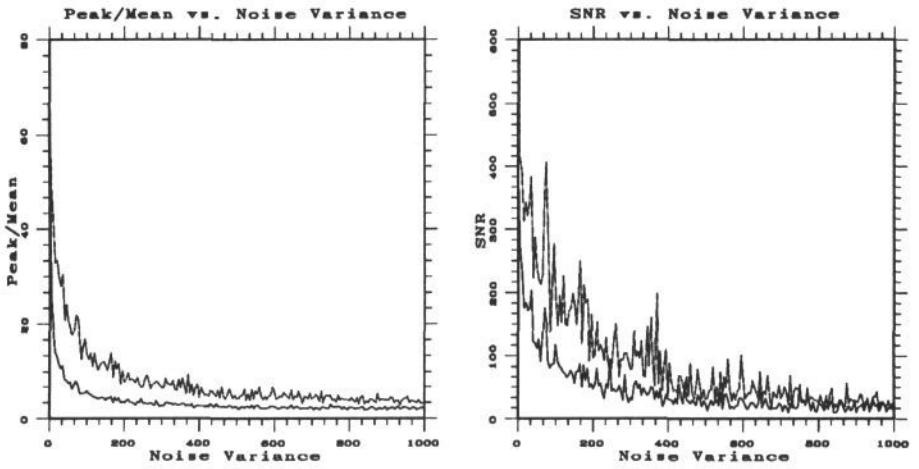

(a) Peak to mean ratio *(b) $(Peak\text{-}Mean)^2$ / Variance*

Figure 5. Energy and Coherent CHT accumulator array responses to circle image and noise (coherent CHT is the top trace in both cases).

The last set of results in this section, Figures 6, show cross-sections through the peaks in the accumulator arrays, taken at the known y-value of the circle centre, for a limited number of input image noise variances.

4.3 Accumulator arrays

The final set of results shows examples of the Energy and Coherent CHT accumulator arrays. Figure 7 shows the accumulator array for the Energy CHT and 8 shows the accumulator array for the Coherent CHT.

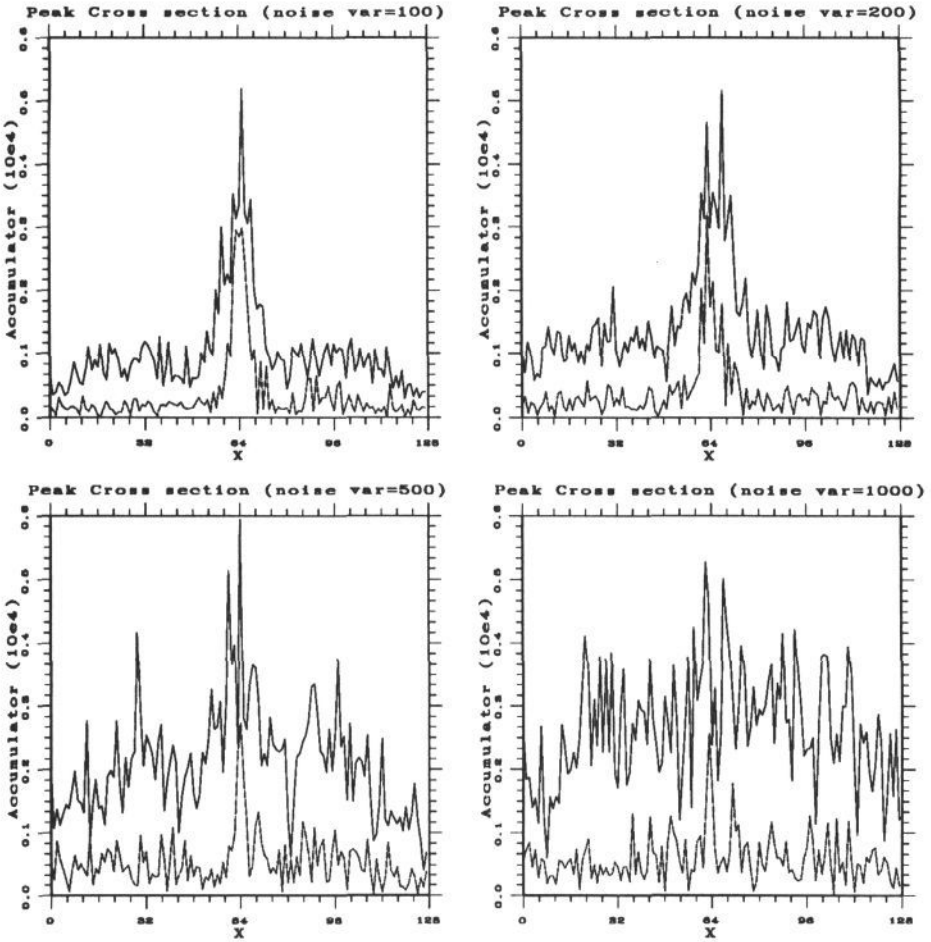

Figure 6. Peak widths for circle image with noise variances $\sigma_i^2 = 100, 200, 500, 1000$ *. (Energy CHT is the upper trace in all cases)*

5 Discussion

We consider the comparative performance of the Energy and Coherent CHT techniques. The quantitative experimental work uses images containing either noise alone or a single isolated circle with added noise We distinguish between noise of this sort (additive, zero-mean, and Gaussian) and clutter (interference effects between multiple objects, Bar-Shal 1988, Yuen 1990). The response of the Energy and Coherent CHT's to noise alone provides an indication of the background that any peak due to the presence of a signal will be embedded in.

The CHT processing flow, Figure 3, shows the sequence of operations applied to images. In the quantitative experiments we have controlled the contrast of the circle (it is either present or absent) and have controlled the noise variance, σ_i^2, added to the image. The range was from no noise to σ_i^2=1000.

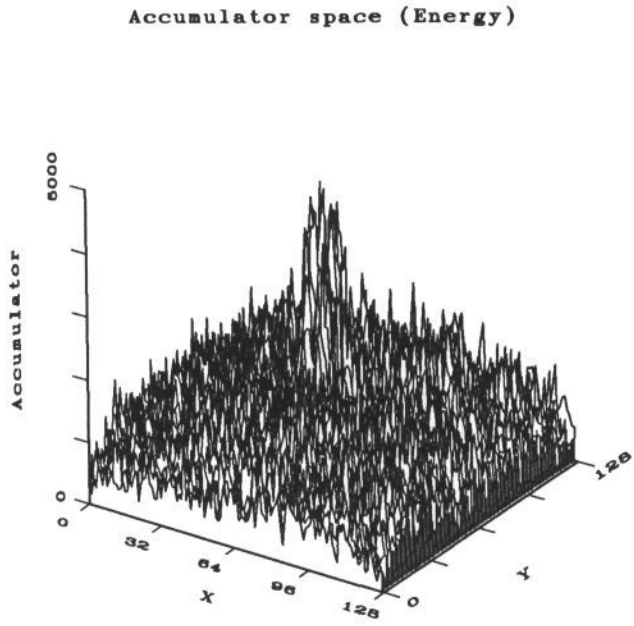

Figure 7. Energy CHT Accumulator array for a circle image with $\sigma_i^2 = 200$

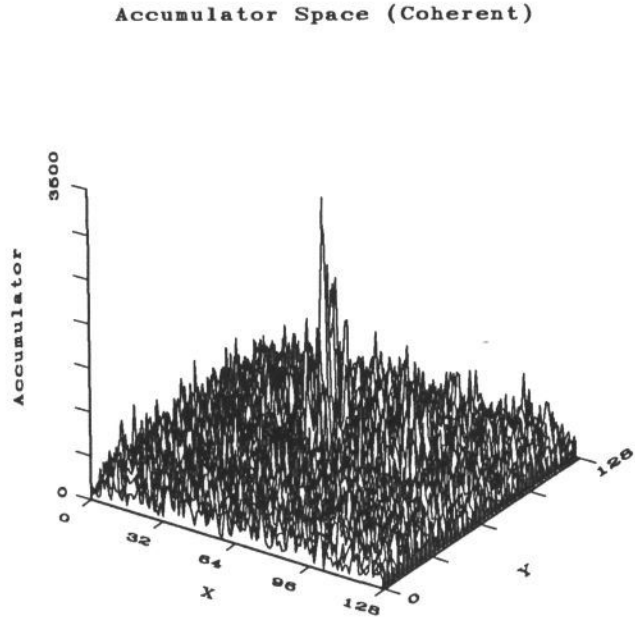

Figure 8. Coherent CHT Accumulator array for a cirlce image with $\sigma_i^2 = 200$

The first operation is a Sobel edge detection that produces separable Cartesian components. The approach taken here would be similar for other edge and orientation detection schemes. The partial derivatives of the image luminance function in the x and y directions, S_X and S_Y respectively, are Gaussian distributed having variance depending on the noise amplification factor of the edge detector (Hamming 1983). For the Sobel this is:

$$\mathrm{var}\{S_x\} = \mathrm{var}\{S_y\} = \sigma_s^2 = 12\sigma_i^2 \tag{8}$$

We convert from Cartesian to Polar to give edge magnitude and orientation. The noise statistics of the edge magnitude are then Rician (Woodward 1964, Levanon 1988). In the absence of a signal the Rician becomes the Rayleigh distribution, and for high high signal to noise ratios it approximates a Gaussian (Levanon 1988). In both cases we can reason about the noise in the edge magnitude that forms the input to both the Energy and Coherent CHT .

5.1 Response to Noise Alone

In the absence of a circular object in the image the edge magnitude will be Rayleigh distributed with mean and variance (Papoulis 1965):

$$E\{e(\mathbf{x})\} = \sqrt{\frac{\pi}{2}}\sigma_s = \sqrt{6\pi}\sigma_i,\ \mathrm{var}\{e(\mathbf{x})\} = 2\left(1-\frac{\pi}{4}\right)\sigma_s^2 = 24\left(1-\frac{\pi}{4}\right)\sigma_i^2 \tag{9}$$

The edge orientation will be uniformly distributed. The number of points within a distance Rmin to R_{max} that have an edge orientation that passes over a pixel (assumed unit area) will be taken as:

$$n_e \approx \sqrt{2}\left(R_{\max} + R_{\min}\right) \tag{10}$$

Energy CHT

Each edge point contributions to a point in the accumulator sum to give the mean and variance of the Energy CHT :

$$E\{H_E(\mathbf{x})\} = n_e\sqrt{6\pi}\sigma_i\ ,\ \ \mathrm{var}\{H_E(\mathbf{x})\} = n_e 24\left(1-\frac{\pi}{4}\right)\sigma_i^2 \tag{11}$$

Coherent CHT

The Coherent CHT accumulator array is complex. In the absence of a circle the components are zero-mean. An estimate of the variance of the components is:

$$\mathrm{var}\{\Re(H_C)\} = \mathrm{var}\{\Im(H_C)\} \approx 12n_e\left(1-\frac{\pi}{4}\right)\sigma_i^2 \tag{12}$$

From the Coherent CHT components we form the Rician distributed magnitude of the response. This is Rayleigh distributed in the absence of any signal, with mean and variance:

$$E\{|H_C|\} \approx \left[6\pi n_e\left(1-\frac{\pi}{4}\right)\right]^{\frac{1}{2}}\sigma_i,\ \mathrm{var}\{|H_C|\} \approx 24n_e\left(1-\frac{\pi}{4}\right)^2\sigma_i^2 \tag{13}$$

The analysis confirms the observation, ceteris paribus, that the mean background level for the Energy CHT is greater than that for the Coherent CHT. The background increases with the area of the annulus within R_{min} and R_{max} for the Energy CHT, whereas it increases only with the square root of this area for the Coherent CHT. A lower variance for the Coherent CHT is predicted by the scale factor $\left(1-\frac{\pi}{4}\right) \approx 0.2$ for the Energy and $\left(1-\frac{\pi}{4}\right)^2 \approx 0.05$ for the Coherent CHT.

5.2 Circle plus Noise Behaviour

We seek the width of the peak in the accumulator array when the circle is present in the image. The contribution to the peak from the points on the edge of the circle are considered in isolation from the background pedestal. We will examine the peak for the Energy CHT using a slightly different approach to Davies (Davies 1992), we are dealing with "spokes" that cover a range of radii rather than a single radius. From the Energy CHT result we make reasoned predictions about the peak in the Coherent CHT case, a more rigorous analysis is in progress.

We will use the high SNR approximation that the edge magnitude and orientation are Gaussian distributed. We seek the peak distribution in the accumulator array at the centre of the circle where the "spokes" intersect. We make the approximation that the width of the "spoke" is constant along its length, being the width near the centre of the circle. The probability that all the spokes pass through the point **x** is then:

$$P(\mathbf{x}) = \prod_{\theta=0}^{2\pi} \frac{1}{2\pi\sigma_w^2} \exp\left[-\frac{\left(\hat{\mathbf{n}}_\perp^T \mathbf{x}\right)^2}{2\sigma_w^2}\right] = \frac{1}{2\pi\sigma_w^2} \exp\left[-\frac{\sum_{\theta=0}^{2\pi}\left(\hat{\mathbf{n}}_\perp^T \mathbf{x}\right)^2}{2\sigma_w^2}\right] \qquad (14)$$

where σ_w^2 is the variance of the width of the spoke near the centre of the circle, $\hat{\mathbf{n}}_\perp$ is the unit vector perpendicular to the spoke, and θ is the angle the spoke makes with the x-axis. Replacing the summation over a circle with an integral this is $\|\mathbf{x}\|^2 \int_0^{2\pi} \sin^2\theta d\theta$ which has the value πr^2 where r is the distance from the centre of the circle. The probability distribution for all the spokes passing through a point at **x** at a distance r from the centre of the circle then becomes:

$$P(r) = \frac{1}{2\pi\sigma_w^2} \exp\left[-\frac{\pi r^2}{2\sigma_w^2}\right] = \frac{E}{24\pi R^2 \sigma_i^2} \exp\left[-\frac{\pi E^2 r^2}{24 R^2 \sigma_i^2}\right] \qquad (15)$$

where E is the edge strength and R the true radius of the circle.

For the Coherent CHT we have to consider constructive and destructive interference. Spokes from opposite sides of the circle are in phase at the centre but in anti-phase a distance $\lambda/4$ from the centre. In the experiments reported here this is a distance of 4 pixels. This is confirmed qualitatively by the narrowing of the Coherent CHT peak visible in Figure 6 where it can be compared with the peak widths of the Energy CHT.

6 Conclusions

We have introduced the Coherent Circle Hough Transform and its novel use of phase to code for radii. The comparative results show clearly that the background mean and variance levels in the Energy CHT accumulator array are larger than for the Coherent CHT. The widths of the observed peaks for the Energy CHT are again broader than those for the Coherent CHT. The peak width for the Energy CHT has been modelled analytically, and the reason for the narrower peak of the Coherent CHT suggested. Further analytical work should reveal the full properties of the Coherent CHT. The experimental work reported here indicates that for the detection of isolated circles in additive noise the Coherent CHT is a superior technique when compared with the conventional Energy CHT.

REFERENCES

Atherton 1990. Atherton, T.J., Nudd, G.R., Kerbyson, D.J., et. al. Detection and Segmentation of Blobs using the Warwick Multiple-SIMD Architecture. In Parallel Architectures for Image Processing, SPIE, February 1990, pp. 96-104.

Ballard 1982. Ballard, D.H. & Brown, C.M. Computer Vision, Prentice-Hall , 1982.

Bar-Shal 1988. Bar-Shalom, Y. & Fortmann, T.E. Tracking and Data Association, Vol. 179, Academic Press, Mathematics in Science and Engineering, 1988.

Davies 1988. Davies, E.R. A Modified Hough Scheme for General Circle Location . Pattern Recognition Letters January 1988; 7, pp. 37-43.

Davies 1992. Davies, E.R. Modelling Peak Shapes Obtained by Hough Transform. IEE Proceedings-E January 1992; 139 (1), pp. 9-12.

Duda 1972. Duda, R.O. & Hart, P.E. Use of the Hough Transform to Detect Lines and Curves in Pictures. CACM January 1972; 15 (1), pp. 11-15.

Hamming 1983 Hamming, R.W. Digital Filters, Prentice-Hall, 1983.

Kimme 1975. Kimme, C., Ballard, D., & Sklansky, J. Finding Circles by an Array of Accumulators. Proc. ACM 1975; 18 (2), pp. 120-122.

Langley 1990. Langley, K., Atherton, T.J., Wilson, R.G., & Larcombe, M.H.E. Vertical and Horizontal Disparities from Phase. In ECCV 90, Antibes, Spinger-Verlag, April 1990.

Langley 1992. Langley, K., Fleet, D.J., & Atherton, T. Multiple Motions from Instantaneous Frequency. In Proc. CVPR '92, IEEE, 1992, pp. 846-849.

Leavers1992 Leavers, V.F., Shape Detection in Computer Vision using the Hough Transform, Springer-Verleg, 1992.

Levanon 1988. Levanon, N. Radar Principles, Wiley , 1988.

Minor 1981. Minor, L.G. & Sklansky, J. Detection and Segmentation of blobs in infrared images. IEEE Trans. SMC 1981; 11, pp. 194-201.

Papoulis 1965. Papoulis, A. Probability, Random Variables, and Stochastic Processes, McGraw-Hill, Polytechnic Institute of Brooklyn, 1965.

Sklansky 1978. Sklansky, J. On the Hough Technique for Curve Detection. IEEE Trans. on Computers October 1978; C-27 (10), pp. 923-926.

Wilson 1992. Wilson, R.G., Calway, A.D., & Knutsson, H. Multiresolution estimation of 2-d disparity using a frequency domain approach. In Proc. of the BMVC, 1992, pp. 227-236.

Woodward 1964 Woodward, P.M. Probability and Information Theory, with Applications to Radar, Pergamon, 1964.

Yuen 1989. Yuen, H.K., Princen, J., Illingworth, J., & Kittler, J. A Comparative Study of Hough Transform Methods for Circle Finding. In Proc. AVC, 1989, pp. 169-174.

Yuen 1990. Yuen, H.K., Princen, J., Illingworth, J., & Kittler, J. Comparative study of Hough Transform methods for circle finding. IVC February 1990; 8 (1), pp. 71-77.